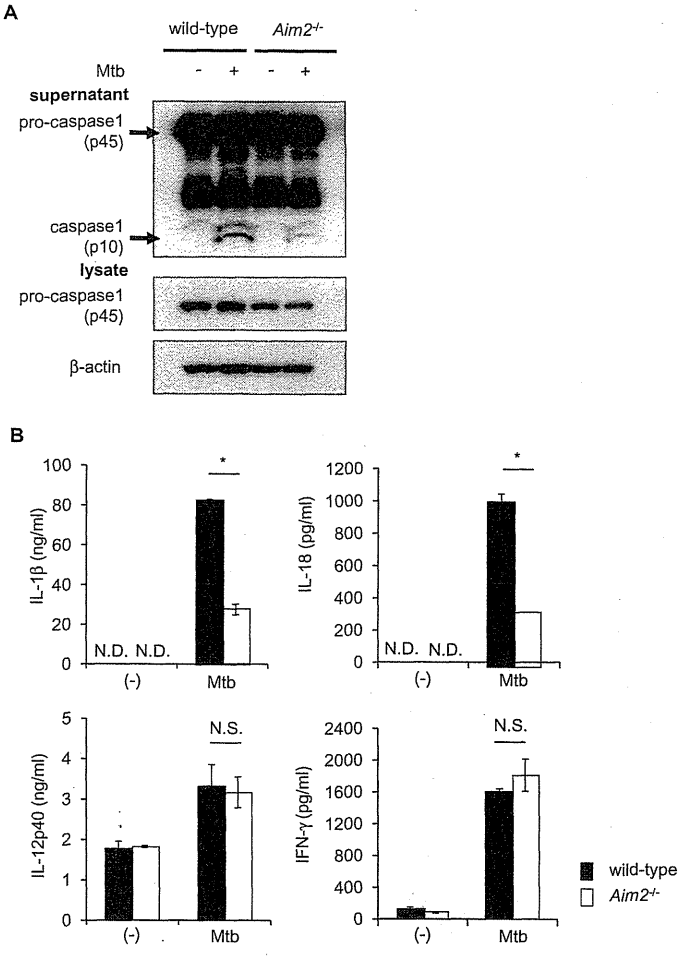

Fig. 4. AIM2-dependent inflammasome activation in *M. tuberculosis* infection. (A) *M. tuberculosis*-infected peritoneal macrophage culture supernatants were immuno-precipitated and the cell pellets were lysed. Caspase-1 specific bands were detected by western blotting and β-actin was used as a control for the cell lysate. One representative of three independent experiments is shown. (B) Thioglycollate-induced peritoneal macrophages were infected with *M. tuberculosis* (MOI of 3). The levels of the indicated cytokines in the culture supernatants were measured by ELISA. Data are presented as means ± SD of triplicate determinants and are one representative of three independent experiments. *, $P < 0.01$. N.S., not significant; N.D., not detected.

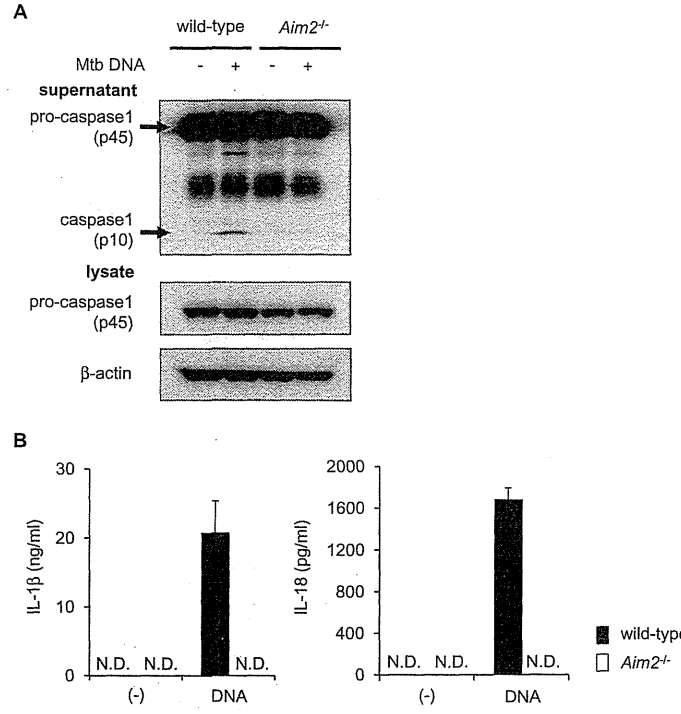

Fig. 5. AIM2 inflammasome is activated by *M. tuberculosis* genomic DNA. (A) Peritoneal macrophages were stimulated with LPS and transfected with Mtb DNA using Lipofectamine 2000. The culture supernatants were immuno-precipitated and the cells were lysed. Caspase-1 specific bands were detected by western blotting. β-actin was used as a control for the cell lysate. One representative of three independent experiments is shown. (B) Thioglycollate-elicited peritoneal macrophages were stimulated with LPS and transfected with Mtb DNA using Lipofectamine 2000. The production of IL-1β and IL-18 in the culture supernatants was measured by ELISA. Data are presented as means ± SD of triplicate determinants and are one representative of three independent experiments. N.D., not detected.

M. tuberculosis (Mtb DNA) activates caspase-1. Mtb DNA was transfected into the cytoplasm of peritoneal macrophages primed with LPS and analyzed for caspase-1 activation (Fig. 5A). The cleaved p10 form of caspase-1 was detected in LPS/Mtb DNA-stimulated wild-type macrophages. In contrast, the active form of caspase-1 was not induced in *Aim2*$^{-/-}$ macrophages stimulated with LPS/Mtb DNA. We also analyzed the secretion of IL-1β and IL-18 (Fig. 5B). Wild-type peritoneal macrophages stimulated with LPS/Mtb DNA secreted substantial amounts of IL-1β and IL-18. In contrast, the production of IL-1β and IL-18 was profoundly reduced in *Aim2*$^{-/-}$ macrophages. These findings indicate that AIM2 mediates Mtb DNA-dependent induction of caspase-1 activation and subsequent IL-1β/IL-18 secretion.

Mycobacterium tuberculosis genomic DNA is co-localized with cytosolic AIM2

We next determined the cellular compartment where Mtb DNA is recognized by AIM2. Recent studies demonstrated that virulent *M. tuberculosis* escapes from phagosomes into the cytosol (43). *Mycobacterium tuberculosis* was incubated with Hoechst 33342 to label genomic DNA and then infected into RAW264.7 macrophages. Some Mtb DNA was not co-localized with Rab7, which is recruited to the phagosomal membrane (Fig. 6A). Although LAMP1 is enriched in the phagolysosomal compartment, some Mtb DNA was not co-localized with it (Fig. 6B, upper panels). In contrast, genomic DNA from non-virulent *M. bovis* bacillus Calmette-Guerin (BCG) was fully merged with phagosome markers, Rab7 and LAMP1 (Supplementary Figure 4 is available at *International Immunology* Online). These findings indicate that Mtb DNA is present in the cytosol. We further visualized cytosolic AIM2 (Fig. 6B, lower panels). Mtb DNA, which was not present within the phagosome, co-localized with AIM2. We also analyzed co-localization of AIM2 and Mtb DNA in peritoneal macrophages (Supplementary Figure 5 is available at *International Immunology* Online). As was the case in RAW264.7 macrophages, Mtb DNA was merged with

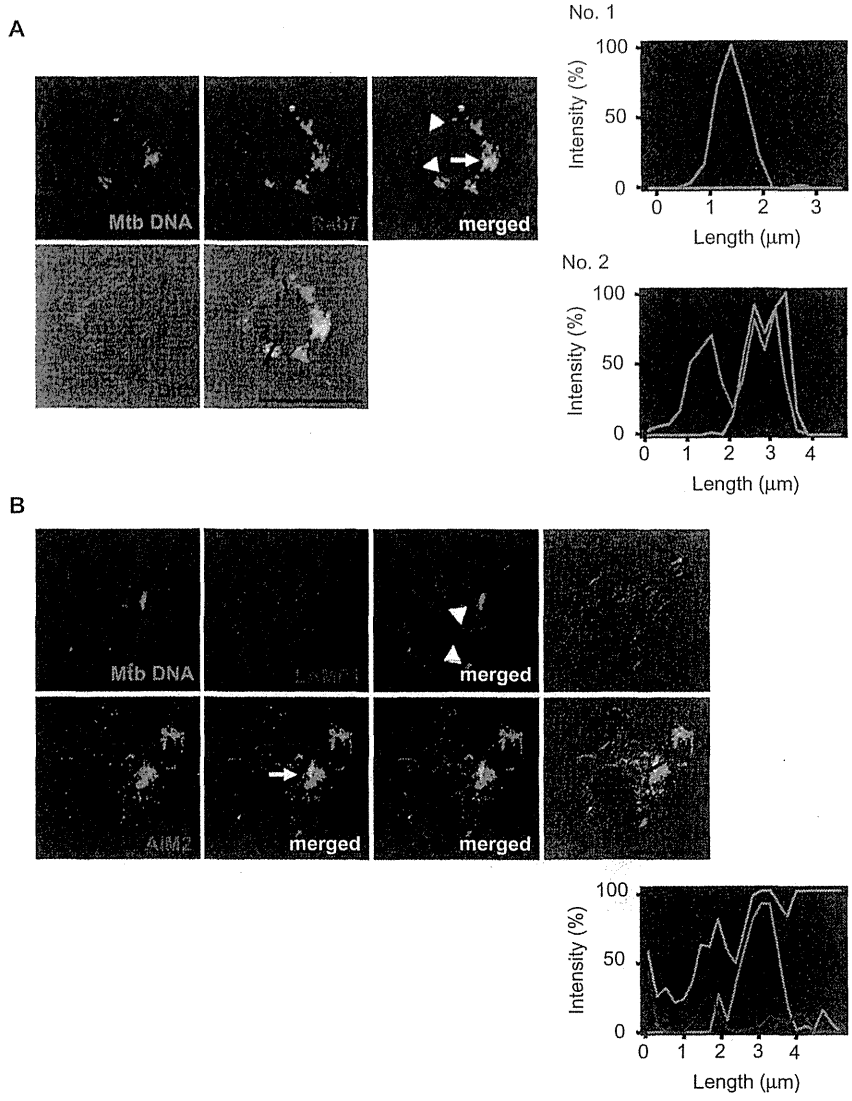

Fig. 6. Co-localization of cytosolic *M. tuberculosis* genomic DNA with AIM2. (A) RAW264.7 macrophages were infected with Hoechst-labeled *M. tuberculosis* (red) and stained with antibody to Rab7 (green). Scale bar represents 20 μm. Arrow heads indicate localization of the red signal alone. Arrow indicates co-localization of the red and green signals. Fluorescence intensities of the red and green signals were quantified along selected lines 1 or 2 (no. 1, upper panel; no. 2, lower panel). (B) RAW264.7 macrophages were infected with Hoechst-labeled *M. tuberculosis* (red) and stained with antibody to LAMP1 (blue, upper panels) or AIM2 (green, lower panels). Scale bar represents 20 μm. Arrow heads indicate localization of the red signal alone. Arrow indicates co-localization of the red and green signals. Fluorescence intensities of the blue, red and green signals were quantified along a selected line.

AIM2, but not with LAMP1. These findings demonstrate that the recognition of Mtb DNA by AIM2 occurs within the cytosolic compartment.

Discussion

In this study, we analyzed the role of AIM2 in the host defense against *M. tuberculosis* using AIM2-deficient mice. *Aim2*$^{-/-}$ mice were highly susceptible to mycobacterial infection compared with wild-type mice and showed severely reduced production of IL-1β and IL-18. IL-1β plays an important role in anti-mycobacterial host defense responses (22–26), and IL-18 is responsible for resistance to *M. tuberculosis* infection via induction of IFN-γ-mediated T_h1 responses (27–29). Therefore, defective production of IL-1 family cytokines, such as IL-1β and IL-18, might cause a high sensitivity to *M. tuberculosis* infection in *Aim2*$^{-/-}$ mice.

Mycobacterium tuberculosis has been shown to activate the inflammasome via NLRP3 (15–18). However, several studies showed that mice deficient in NLRP3 are not highly sensitive to *M. tuberculosis* infection (26, 30–32). This study clearly shows that *Aim2*$^{-/-}$ mice are highly sensitive to infection with *M. tuberculosis* with defective activation of caspase-1, identifying AIM2 as the important molecule for activation of the inflammasome in *M. tuberculosis* infection. However, mice deficient in ASC or caspase-1,

critical components of the inflammasome, do not show dramatically severe phenotypes as compared with those of IL-1β-deficient mice in *M. tuberculosis* infection (25, 26). In this regard, AIM2 might also activate a signaling pathway, leading to inflammasome-independent production of the IL-1 family of cytokines. *Mycobacterium tuberculosis*-infected *Aim2*$^{-/-}$ macrophages expressed high amounts of IFN-β, confirming a previous study that showed that poly(dA:dT) induces increased amounts of IFN-β in *Aim2*$^{-/-}$ splenocytes and macrophages (37). Thus, AIM2 might be involved in the signaling pathway responsible for suppression of IFN-β. IFN-β is induced by *M. tuberculosis* infection and then suppresses the production of IL-1β in macrophages and dendritic cells (44,45). Indeed, the type I IFNs have been shown to contribute to impaired host resistance to *M. tuberculosis* in mice (26, 46–48). Thus, it is possible that AIM2 activates two signaling pathways, one mediating the inflammasome-dependent processing of the IL-1 family of cytokines and a second that mediates activation of unknown pathways that sustain the production of IL-1β by suppressing type I IFNs.

The cleaved p10 form of caspase-1 was not detected, and production of IL-1β and IL-18 was almost completely abrogated in Mtb DNA-stimulated *Aim2*$^{-/-}$ macrophages. In contrast, IL-1β and IL-18 were moderately produced and the cleaved form of caspase-1 was also slightly detected in *M. tuberculosis*-infected *Aim2*$^{-/-}$ peritoneal macrophages. This might be due to NLRP3-dependent recognition of *M. tuberculosis* (15–18). An AIM2-independent and inflammasome-independent mechanism for IL-1β release might also be operating in mycobacterial infection. Matrix metalloproteinase-9 (MMP-9, also known as gelatinase B) is robustly induced in mycobacteria-infected macrophages, causing inactive IL-1β to be processed into a biologically active form (49, 50). Thus, MMP-9 might be involved in the inflammasome-independent processing of the IL-1 family of cytokines during *M. tuberculosis* infection.

We showed that Mtb DNA co-localized with AIM2 in the cytosol, but the localization of mycobacteria within macrophages is still under debate (51). Virulent *M. tuberculosis* resides within phagosomes by inhibiting their maturation into phagolysosomes (52–54). But there are several reports supporting cytosolic escape of virulent mycobacteria (43, 51, 55–57). *Mycobacterium marinum* can escape from phagosomes into the cytosol by actin-based motility (55), an activity which depends on the region of difference 1 [RD1 (57)]. *Mycobacterium tuberculosis* and *Mycobacterium leprae* can translocate from phagosomes to the cytosol of myeloid cells in an RD1-dependent manner and following cell death (43). This might be compatible with our results for *M. tuberculosis*-induced activation of the AIM2 inflammasome, which also requires induction of pyroptosis, a form of cell death (33–39). Our data suggest that *M. bovis* BCG, lacking the RD1 locus, fails to escape from phagosomes into the cytosol. In addition, *M. bovis* BCG does not induce IL-1β secretion from macrophages (32). Thus, AIM2 recognizes *M. tuberculosis* upon translocation into the cytosol. It will be interesting to determine how Mtb DNA becomes exposed and is recognized by AIM2 in the cytosol.

We have identified a novel recognition mechanism in mycobacterial infection through the cytosolic DNA sensor AIM2. Several pattern recognition receptors, such as TLRs and C-type lectin receptors mediate gene expression in mycobacterial infection. AIM2 is co-operatively involved in the immune response to mycobacterial infection with these innate immune mycobacterial sensors.

Supplementary data

Supplementary data are available at *International Immunology* Online.

Funding

This work was supported by Core Research for Evolutional Science and Technology, Japan Science and Technology Agency; Grant-in-Aid from the Ministry of Education, Culture, Sports, Science and Technology; Grant-in-Aid from the Ministry of Health, Labour, and Welfare; and the Osaka Foundation for the Promotion of Clinical Immunology.

Acknowledgements

We thank C. Hidaka for secretarial assistance and Y. Magota for technical assistance.

References

1 Kaufmann, S. H. E. and McMichael, A. J. 2005. Annulling a dangerous liaison: vaccination strategies against AIDS and tuberculosis. *Nat. Med.* 11:33.
2 Ferwerda, G., Kullberg, B. J., de Jong, D. J. *et al.* 2007. *Mycobacterium paratuberculosis* is recognized by Toll-like receptors and NOD2. *J. Leukoc. Biol.* 82:1011.
3 Yang, Y., Yin, C., Pandey, A. *et al.* 2007. NOD2 pathway activation by MDP or *Mycobacterium tuberculosis* infection involves the stable polyubiqutination of Rip2. *J. Biol. Chem.* 282:36223.
4 Hemmi, H., Takeuchi, O., Kawai, T. *et al.* 2000. A Toll-like receptor recognizes bacterial DNA. *Nature* 408:740.
5 Takeuchi, O. and Akira, S. 2010. Pattern recognition receptors and inflammation. *Cell* 140:805.
6 Geijtenbeek, T. B., Van Vliet, S. J., Koppel, E. A. *et al.* 2003. Mycobacteria target DC-SIGN to suppress dendritic cell function. *J. Exp. Med.* 197:7.
7 Kang, P. B., Azad, A. K., Torrelles, J. B. *et al.* 2005. The human macrophage mannose receptor directs *Mycobacterium tuberculosis* lipoarabinomannan-mediated phagosome biogenesis. *J. Exp. Med.* 202:987.
8 Ishikawa, E., Ishikawa, T., Morita, Y. S. *et al.* 2009. Direct recognition of the mycobacterial glycolipid, trehalose dimycolate, by C-type lectin Mincle. *J. Exp. Med.* 206:2879.
9 Ferwerda, G., Girardin, S. E., Kullberg, B. J. *et al.* 2005. NOD2 and toll-like receptors are nonredundant recognition systems of *Mycobacterium tuberculosis*. *PLoS Pathog.* 1:279.
10 Divangahi, M., Mostowy, S., Coulombe, F. *et al.* 2008. NOD2-deficient mice have impaired resistance to *Mycobacterium tuberculosis* infection through defective innate and adaptive immunity. *J. Immunol.* 181:7157.
11 Martinon, F., Burns, K. and Tschopp, J. 2002. The inflammasome: a molecular platform triggering activation of inflammatory caspases and processing of proIL-β. *Mol. Cell.* 10:417.
12 Agostini, L., Martinon, F., Burns, K. *et al.* 2004. NALP3 forms an IL-1β-processing inflammasome with increased activity in Muckle-Wells autoinflammatory disorder. *Immunity* 20:319.
13 Martinon, F., Mayor, A. and Tschopp, J. 2009. The inflammasomes: guardians of the body. *Annu. Rev. Immunol.* 27:229.

14 Schroder, K. and Tschopp, J. 2010. The inflammasomes. *Cell* 140:821.
15 Koo, I. C., Wang, C., Raghavan, S. *et al.* 2008. ESX-1-dependent cytolysis in lysosome secretion and inflammasome activation during mycobacterial infection. *Cell Microbiol.* 10:1866.
16 Carlsson, F., Kim, J., Dumitru, C. *et al.* 2010. Host-detrimental role of Esx-1-mediated inflammasome activation in mycobacterial infection. *PLoS Pathog.* 6:e1000895.
17 Mishra, B. B., Moura-Alves, P., Sonawane, A. *et al.* 2010. *Mycobacterium tuberculosis* protein ESAT-6 is a potent activator of the NLRP3/ASC inflammasome. *Cell Microbiol.* 12:1046.
18 Wong, K. W. and Jacobs, W. R. Jr. 2011. Critical role for NLRP3 in necrotic death triggered by *Mycobacterium tuberculosis. Cell Microbiol.* 13:1371.
19 Van de Veerdonk, F. L., Netea, M. G., Dinarello, C. A. and Joosten, L. A. 2011. Inflammasome activation and IL-1β and IL-18 processing during infection. *Trends Immunol.* 32:110.
20 Dinarello, C. A. 1996. Biologic basis for interleukin-1 in disease. *Blood* 87:2095.
21 Dinarello, C. A. 1999. IL-18: a TH1-inducing, proinflammatory cytokine and new member of the IL-1 family. *J. Allergy Clin. Immunol.* 103:11.
22 Yamada, H., Mizumo, S., Horai, R., Iwakura, Y. and Sugawara, I. 2000. Protective role of interleukin-1 in mycobacterial infection in IL-1α/β double-knockout mice. *Lab. Invest.* 80:759.
23 Juffermans, N. P., Florquin, S., Camoglio, L. *et al.* 2000. Interleukin-1 signaling is essential for host defense during murine pulmonary tuberculosis. *J. Infect. Dis.* 182:902.
24 Fremond, C. M., Togbe, D., Doz, E. *et al.* 2007. IL-1 receptor-mediated signal is an essential component of MyD88-dependent innate response to *Mycobacterium tuberculosis* infection. *J. Immunol.* 179:1178.
25 Mayer-Barber, K. D., Barber, D. L., Shenderov, K. *et al.* 2011. Caspase-1 independent IL-1β production is critical for host resistance to *Mycobacterium tuberculosis* and does not require TLR signaling in vivo. *J. Immunol.* 184:3326.
26 Cooper, A. M., Mayer-Barber, K. D. and Sher, A. 2011. Role of innate cytokines in mycobacterial infection. *Mucosal Immunol.* 4:252.
27 Sugawara, I., Yamada, H., Kaneko, H. *et al.* 1999. Role of interleukin-18 (IL-18) in mycobacterial infection in IL-18-gene-disrupted mice. *Infect. Immun.* 67:2585.
28 Schneider, B. E., Korbel, D., Hagens, K. *et al.* 2010. A role for IL-18 in protective immunity against *Mycobacterium tuberculosis. Eur. J. Immunol.* 40:396.
29 Takeda, K., Tsutsui, H., Yoshimoto, T. *et al.* 1998. Defective NK cell activity and Th1 response in IL-18-deficient mice. *Immunity* 8:383.
30 Walter, K., Hölscher, C., Tschopp, J. and Ehlers, S. 2010. NALP3 is not necessary for early protection against experimental tuberculosis. *Immunobiology* 215:804.
31 McElvania Tekippe, E., Allen, I. C., Hulseberg, P. D. *et al.* 2010. Granuloma formation and host defense in chronic *Mycobacterium tuberculosis* infection requires PYCARD/ASC but not NLRP3 or caspase-1. *PLoS One* 5:e12320.
32 Dorhoi, A., Nouailles, G., Jörg, S. *et al.* 2012. Activation of the NLRP3 inflammasome by *Mycobacterium tuberculosis* is uncoupled from susceptibility to active tuberculosis. *Eur. J. Immunol.* 42:374.
33 Bürckstümmer, T., Baumann, C., Blüml, S. *et al.* 2009. An orthogonal proteomic-genomic screen identifies AIM2 as a cytoplasmic DNA sensor for the inflammasome. *Nat. Immunol.* 10:266.
34 Hornung, V., Ablasser, A., Charrel-Dennis, M. *et al.* 2009. AIM2 recognizes cytosolic dsDNA and forms a caspase-1-activating inflammasome with ASC. *Nature* 458:514.
35 Fernandes-Alnemri, T., Yu, J. W., Datta, P., Wu, J. and Alnemri, E. S. 2009. AIM2 activates the inflammasome and cell death in response to cytoplasmic DNA. *Nature* 458:509.
36 Roberts, T. L., Idris, A., Dunn, J. A. *et al.* 2009. HIN-200 proteins regulate caspase activation in response to foreign cytoplasmic DNA. *Science* 323:1057.
37 Rathinam, V. A. K., Jiang, Z., Waggoner, S. N. *et al.* 2010. The AIM2 inflammasome is essential for host defense against cytosolic bacteria and DNA viruses. *Nat. Immunol.* 11:395.
38 Fernandes-Alnemri, T., Yu, J. W., Juliana, C. *et al.* 2010. The AIM2 inflammasome is critical for innate immunity to *Francisella tularensis. Nat. Immunol.* 11:385.
39 Jones, J. W., Kayagaki, N., Broz, P. *et al.* 2010. Absent in melanoma 2 is required for innate immune recognition of *Francisella tularensis. Proc. Natl. Acad. Sci. USA* 107:9771.
40 Warren, S. E., Armstrong, A., Hamilton, M. K. *et al.* 2010. Cytosolic bacterial DNA activates the inflammasome via Aim2. *J. Immunol.* 185:818.
41 Tsuchiya, K., Hara, H., Kawamura, I. *et al.* 2010. Involvement of absent in melanoma 2 in inflammasome activation in macrophages infected with *Listeria monocytogenes. J. Immunol.* 185:1186.
42 Kleinnijenhuis, J., Joosten, L. A., van de Veerdonk, F. L. *et al.* 2009. Transcriptional and inflammasome-mediated pathways for the induction of IL-1β production by *Mycobacterium tuberculosis. Eur. J. Immunol.* 39:1914.
43 van der Wel, N., Hava, D., Houben, D. *et al.* 2007. *M. tuberculosis* and *M. leprae* translocate from the phagolysosome to the cytosol in myeloid cells. *Cell* 129:1287.
44 Novikov, A., Cardone, M., Thompson, R. *et al.* 2011. *Mycobacterium tuberculosis* triggers host type I IFN signaling to regulate IL-1β production in human macrophages. *J. Immunol.* 187:2540.
45 Mayer-Barber, K. D., Andrade, B. B., Barber, D. L. *et al.* 2011. Innate and adaptive interferons suppress IL-1α and IL-1β production by distinct pulmonary myeloid subsets during *Mycobacterium tuberculosis* infection. *Immunity* 35:1023.
46 Stanley, S. A., Johndrow, J. E., Manzanillo, P. and Cox, J. S. 2007. The Type I IFN response to infection with *Mycobaterium tuberculosis* requires ESX-1-mediated secretion and contributes to pathogenesis. *J. Immunol.* 178:3143.
47 Manca, C., Tsenova, L., Bergtold, A. *et al.* 2001. Virulence of a *Mycobacterium tuberculosis* clinical isolate in mice is determined by failure to induce Th1 type immunity and is associated with induction of IFN-α/β. *Proc. Natl. Acad. Sci. USA* 98:5752.
48 Ordway, D., Henao-Tamayo, M., Harton, M. *et al.* 2007. The hypervirulent *Mycobacterium tuberculosis* strain HN878 induces a potent TH1 response followed by rapid down-regulation. *J. Immunol.* 179:522.
49 Schönbeck, U., Mach, F. and Libby, P. 1998. Generation of biologically active IL-1β by matrix metalloproteinases: a novel caspase-1-independent pathway of IL-1β processing. *J. Immunol.* 161:3340.
50 Quiding-Järbrink, M., Smith, D. A. and Bancroft, G. J. 2001. Production of matrix metalloproteinases in response to mycobacterial infection. *Infect. Immun.* 69:5661.
51 Welin, A. and Lerm, M. 2011. Inside or outside the phagosome? The controversy of the intracellular localization of *Mycobacterium tuberculosis. Tuberculosis.* 92:113.
52 Clemens, D. L. and Horwitz, M. A. 1995. Characterization of the *Mycobacterium tuberculosis* phagosome and evidence that phagosomal maturation is inhibited. *J. Exp. Med.* 181:257.
53 Via, L. E., Deretic, D., Ulmer, R. J. *et al.* 1997. Arrest of mycobacterial phagosome maturation is caused by a block in vesicle fusion between stages controlled by rab5 and rab7. *J. Biol. Chem.* 272:13326.
54 Rohde, K., Yates, R. M., Purdy, G. E. and Russell, D. G. 2007. *Mycobacterium tuberculosis* and the environment within the phagosome. *Immunol. Rev.* 219:37.
55 Stamm, L. M., Morisaki, J. H., Gao, L. Y. *et al.* 2003. *Mycobacterium marinum* escapes from phagosomes and is propelled by actin-based motility. *J. Exp. Med.* 198:1361.
56 Gao, L. Y., Guo, S., McLaughlin, B. *et al.* 2004. A mycobacterial virulence gene cluster extending RD1 is required for cytolysis, bacterial spreading and ESAT-6 secretion. *Mol. Microbiol.* 53:1677.
57 Smith, J., Manoranjan, J., Pan, M. *et al.* 2008. Evidence for pore formation in host cell membranes by ESX-1-secreted ESAT-6 and its role in *Mycobacterium marinum* escape from the vacuole. *Infect. Immun.* 76:5478.

THE JOURNAL OF DERMATOLOGY

doi: 10.1111/1346-8138.12047

The Journal of Dermatology 2012; **40**: 1–9

REVIEW ARTICLE

Laboratory procedures for the detection and identification of cutaneous non-tuberculous mycobacterial infections

Kazue NAKANAGA,[1] Yoshihiko HOSHINO,[1] Rie R. YOTSU,[2] Masahiko MAKINO,[1] Norihisa ISHII[1]

[1]*Leprosy Research Center, National Institute of Infectious Diseases, and* [2]*Department of Dermatology, National Center for Global Health and Medicine, Tokyo, Japan*

ABSTRACT

There is evidence that the incidence of cutaneous non-tuberculous mycobacterial (NTM) infection is increasing worldwide. Novel culture methods and new analytical procedures have led to significant advancements in understanding the origin and progression of NTM infections. Differential identification of NTM isolates is important because culture characteristics and/or sensitivity to anti-mycobacterium drugs vary between different mycobacterial species. In this manuscript, we describe the latest diagnostic techniques for cutaneous NTM infection and show how these methodologies can be used for the diagnosis of Buruli ulcer in Japan.

Key words: 16S rRNA gene, Buruli ulcer, cutaneous infection, non-tuberculous mycobacterial infection, polymerase chain reaction, species identification.

INTRODUCTION

The basis for the increase in the number of cases of cutaneous non-tuberculous mycobacterial (NTM) infection is unknown. It has been attributed to an increase in the total number of these patients or to better detection and/or reporting methods.[1–5] Insight into the origin and progression of NTM infections has been significantly advanced due to the employment of novel methods for the culture and analysis of NTM. However, the diagnosis of a cutaneous NTM infection in less experienced hospitals is occasionally delayed, or not made at all, because the causative agent can be difficult to isolate due to its variety of growth characteristics. To date, most cutaneous NTM infections have been caused by *Mycobacterium marinum*[6,7] or by groups of rapidly growing mycobacterial (RGM) species, but sometimes a rare mycobacterium can cause the disease.[8–10] Different strains of mycobacteria generally exhibit different characteristics in culture and/or sensitivity to anti-mycobacterial drugs. Therefore, accurate identification of the causative agent is important for the treatment of NTM infections. In this manuscript, we describe the latest molecular diagnostic techniques for cutaneous NTM infection and present a case study that used these methodologies for BU diagnosis.

NTM IN DERMATOLOGY

Causative agents of dermatological infections

Approximately 30 mycobacterial species have been identified as causative agents of cutaneous infection (Table 1). These species of mycobacteria, with the exception of the *Mycobacterium tuberculosis* complex and *Mycobacterium leprae*, are classified as NTM. They are categorized into four groups based on their growth rate (slow growing mycobacterial [SGM] and RGM species) and photochromogenicity. The identification of mycobacterial species is now rapid and relatively simple. Some of the pathogens identified as causative agents are used as a designation of the disease (e.g. cutaneous *Mycobacterium massiliense* infection).

Clinical symptoms of cutaneous NTM infection

A number of cutaneous diseases, such as erythema, nodules, erosion and ulcers, have been attributed to NTM infection. The point of entry is thought to be via minute cutaneous wounds in which bacteria are attached. Although a visceral NTM infection may cause cutaneous infection in immunocompromised patients, it is not yet clear how many bacteria are required for pathogenicity. There is usually only one cutaneous lesion; however, multiple skin lesions have been observed when pathogenic microbes spread through the lymph fluid. Most infected skin lesions are on exposed areas such as the hands, feet or face, supporting the premise that small external wounds are the penetration pathway. For example, in cutaneous *M. marinum* infection, also known as fish tank granuloma, approximately 80% of the patients have eruption(s) in finger, hand and/or wrist joints. Patients do not experience the pain or itching usually associated with eruptions, but inflammation does sometimes lead to tenderness and/or spontaneous pain.[11,12]

Correspondence: Kazue Nakanaga, Ph.D., Department of Mycobacteriology, Leprosy Research Center, National Institute of Infectious Diseases, 4-2-1 Aoba, Higashi-Murayama, Tokyo 189-0002, Japan. Email: nakanaga@nih.go.jp

Received 7 September 2011; accepted 24 October 2012.

Table 1. Causative agents of cutaneous mycobacterial infections

Growth rate	Traditional Runyon classification	Species (*Mycobacterium*)	Disease
Slow growers	*M. tuberculosis* complex	*M. tuberculosis* *M. bovis*	Cutaneous tuberculosis
	Group I Photochromogens	*M. kansasii* *M. marinum* *M. simiae*	Non-tuberculous mycobacterial infection
	Group II Scotochromogens	*M. gordonae* *M. scrofulaceum* *M. szulgai* *M. ulcerans* subsp. *shinshuense*[a] *M. ulcerans*[a]	
	Group III Non-photochromogens	*M. avium* *M. haemophilum* *M. intracellulare* *M. xenopi*[b]	
Rapid growers	Group IV Rapid growers	*M. abscessus* *M. chelonae* *M. fortuitum* *M. peregrinum* *M. vaccae*	
Unculturable in artificial medium		*M. leprae*	Hansen's disease (Leprosy)

[a]Yellow pigmentation is sometimes lost after several passages. [b]Non-pigmented colonies during early growth. However, most colonies become yellow with age.

CONVENTIONAL IDENTIFICATION OF CUTANEOUS NTM

Specimens

Pus or skin exudate, skin scrapings and skin biopsies are the major source of samples used to perform both conventional and molecular mycobacterial assays (Table 2).[13,14] Isolates, formalin-fixed and/or formalin-fixed paraffin-embedded sections are also used for analysis. Animal coats, aquatic animals, seawater, tap water and swimming pool water are also used in the search for sources of infection. To date, we have received 90 clinical specimens (swabs and tissues) for NTM detection and identification, 225 cultured colonies for identification, 31 paraffin-embedded specimens for detection and 278 NTM cultured colonies for drug susceptibility assay from April 2009 to March 2011. As we discuss later, we have been using this pipeline since 2006, and these samples were analyzed at least in part to reach the correct identification.

Smear test and pathological test

Swabs containing pus or skin exudate spread on a slide glass is used for the smear tests. Smears are stained (Ziehl–Neelsen [Z-N] or Auramine O staining) and examined by light microscopy or fluorescent microscopy (Fig. 1). Pathology specimens are also stained with Z-N staining (Fig 2).

Culture test

Liquid or solid medium is used to culture samples obtained from swabs containing pus or exudate, skin brushes and skin biopsies. The major liquid medium has a Middlebrook 7H9 Broth base combined with a growth indicator system (Mycobacteria Growth Indicator Tube, MB/BacT).[15,16] Three representative solid media are the egg-based Löwenstein–Jensen,

Table 2. Laboratory procedures to detect and identify cutaneous NTM

Pus or scrapings
PCR
Smear test (Z-N stain)
Culture at room temperature: L-J or Ogawa medium
Culture at 37°C: liquid medium (e.g. MGIT)
Frozen in −20°C
Biopsy samples
PCR
Pathological test (Z-N stain)
Culture at room temperature: L-J or Ogawa medium
Culture at 37°C: liquid medium (e.g. MGIT)
Frozen in −20°C
PCR
Culture
Cultured samples
PCR
DDH
Biochemical assays
Drug susceptibility assays
Paraffin- embedded materials
PCR

DDH, DNA–DNA hybridization; L-J medium, Löwenstein–Jensen medium; MGIT, Mycobacteria Growth Indicator Tube;[15] NTM, non-tuberculous mycobacterial; PCR, polymerase chain reaction; Z-N stain, Ziehl–Neelsen stain.

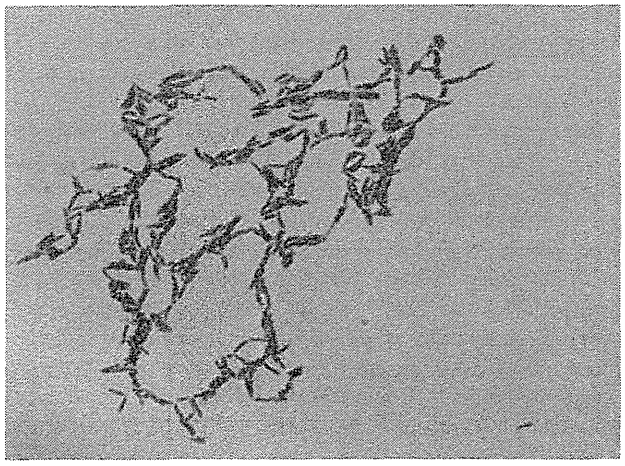

Figure 1. Smear Ziehl–Neelsen staining (original magnification ×1000).

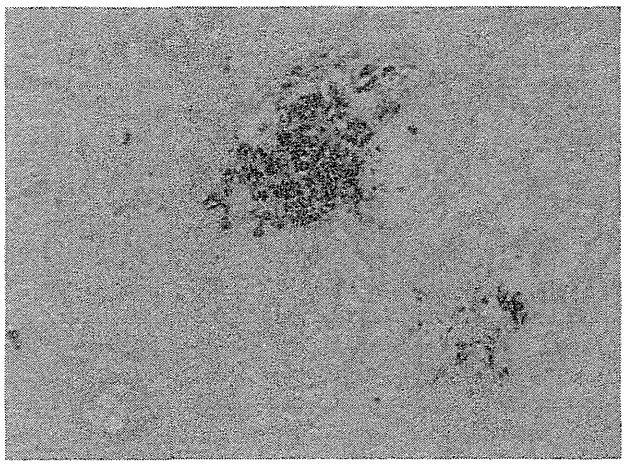

Figure 2. Pathological Ziehl–Neelsen staining (original magnification ×400).

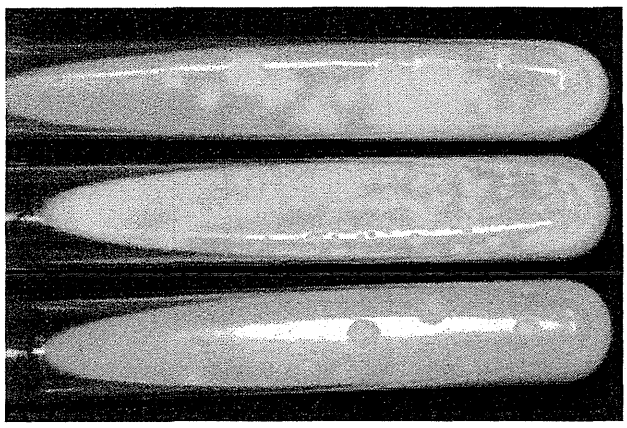

Figure 3. Ogawa medium (culture positive).

Ogawa medium (Fig. 3), or Middlebrook 7H10/7H11 agar medium.[17] Before culturing, pretreatment with Nalc-NaOH is necessary to avoid contamination by other bacteria or fungi. Optimal culturing temperature varies depending on species: 40°C, 37°C, 33°C, 30°C, 28°C and room temperature are frequently used. If multiple incubators are not available for simultaneous use, incubation at 37°C is recommended with simultaneous culturing at room temperature. The isolation period of the causative agents may be shortened when liquid media is used. However, the shortened growth period may not allow sufficient time to observe colony characteristics. Because liquid medium is not suitable for identification when samples contain multiple pathogens, it is recommended that both liquid and solid cultures be grown at the same time.

Biochemical analysis

Biochemical analyses such as the niacin and catalase tests and other enzymatic reaction assays have been the most frequently performed procedures for mycobacterial species identification. These biochemical tests have certain limitations that lead some laboratories to avoid them. For example, testing can only be performed after successful isolation. In addition, running the tests requires complicated quality control and technical expertise.[13,14]

MOLECULAR IDENTIFICATION OF CUTANEOUS NTM

Differential diagnosis by DNA–DNA hybridization (DDH) assays

Differential diagnosis using a commercial kit for mycobacterial DDH can be performed when bacterial isolates are available.[18] The kit contains a panel of 18 major mycobacteria (Table 3). However, it is impossible to diagnose a rare species and subspecies that is not included in the panel, and there have

Table 3. Mycobacterial species identifiable in a commercially available DNA–DNA hybridization test

TB complex (*M. africanum*, *M. bovis*, *M. microti*, *M. tuberculosis*)
M. abscessus
M. avium
M. chelonae
M. fortuitum
M. gastri
M. gordonae
M. intracellulare
M. kansasii
M. marinum
M. nonchromogenicum
M. peregrinum
M. scrofulaceum
M. simiae
M. szulgai
M. terrae
M. triviale
M. xenopi

been several cases of false positives. Attempts to differentiate *Mycobacterium ulcerans* subsp. *shinshuense* (the causative agent of Buruli ulcer [BU] in Japan)[9] from *M. ulcerans* using this kit yield an identification of *M. marinum* (Fig. 4).[19] *Mycobacterium massiliense* and *Mycobacterium bolletii* are misidentified as *Mycobacterium abscessus*,[20] while *Mycobacterium heckeshornense* is classified as *Mycobacterium xenopi*. Additional laboratory procedures are required to discriminate these species. Polymerase chain reaction (PCR) detection of insertion sequence (IS)*2404* can be used to differentiate *M. ulcerans* and/or *M. ulcerans* subsp. *shinshuense* from *M. marinum*.[9,19] However, combination sequence analysis using the *hsp65* and *rpoB* genes is required to separate *M. abscessus*, *M. massiliense* and *M. bolletii*.[20]

Gene amplification assays

Diagnostic genotyping kits for the detection of pathogenic mycobacterial genomes such as *M. tuberculosis*, *Mycobacterium avium*, *Mycobacterium intracellulare* and *Mycobacterium kansasii* are commercially available.[21–23] The correct results

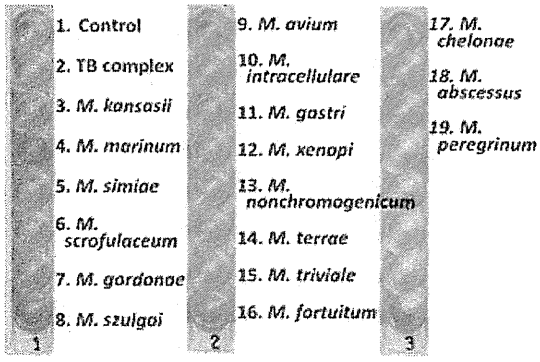

Figure 4. Commercially available DNA–DNA hybridization assay using an *Mycobacterium ulcerans* subsp. *shinshuense* clinical isolate. Blue color change was observed in a well of *M. marinum*.

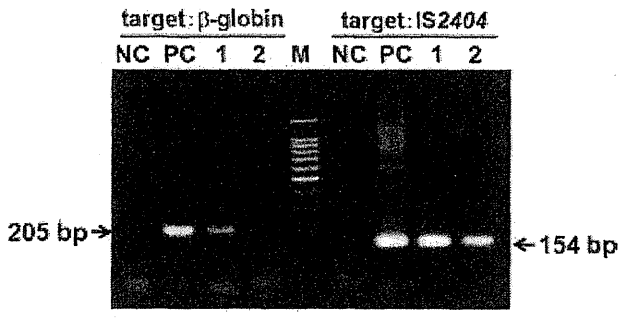

Figure 5. Gel electrophoresis of polymerase chain reaction products amplified using template DNA extracted from formalin-fixed and paraffin-embedded sections. 1, sample 1; 2, sample 2; NC, negative control; PC, positive control.

can be rapidly obtained if certain mycobacteria are present in the specimen material. However, when the results are negative, the smear test and/or culture assays should be performed for the other NTM.

Culturing an SGM can take several weeks. Therefore, genotyping assays such as species-specific PCR (Fig. 5) or 16S rRNA gene sequencing (described below) are extremely effective. Even for RGM species such as *Mycobacterium chelonae*, *M. abscessus* or *Mycobacterium fortuitum*, the primary isolation takes several weeks, but identification can be hastened using genotypic assays in parallel with culture assays. Specimens are sometimes processed into formalin-fixed paraffin-embedded blocks or frozen embedded blocks, making culture assays impossible. The sensitivity and specificity of PCR from these blocks is variable, depending on the condition of the DNA in the specimens. The order of preferred samples for genotypic analysis (from best to worst) is: cultured colonies > fresh specimens > ethanol-fixed specimens > formalin-fixed paraffin-embedded specimens.

Identification using the 16S rRNA gene sequence

If an abundance of bacterial DNA is available, sequence analysis of the first one-third of the 16S rRNA gene (Table 4, primer set; 8F16S-1047R16S) can be used for strain comparisons in the Ribosomal Differentiation of Medical Micro-organisms (RIDOM) database (www.ridom-rdna.de/).[29–31] RIDOM uses the sequence text to find the top 10 reference strains with the highest homology to the query sequence. The sequences contain approximately 500 bp, which includes hypervariable regions A and B of the mycobacterial 16S rRNA gene (*E. coli* positions 54–510). Sequence homology greater than 99% usually leads to a call that two strains are identical. However, this method cannot differentiate between *M. ulcerans* subsp. *shinshuense*, *M. marinum* and *M. ulcerans* due to their sequence similarity. In other cases, *M. kansasii* and *Mycobacterium gastri* exhibit 100% homology in the first 500 bp of their 16S rRNA genes, as do members of the *M. chelonae-abscessus* group.[32,33] These strains require additional methods for differentiation. Sequence analysis of the majority of the 16S rRNA gene (1500 bp) allows differentiation of *M. ulcerans* subsp. *shinshuense*, *M. marinum* and *M. ulcerans* (Table 5).[19,34] The longer sequence read also distinguishes *M. chelonae* from the rest of the *M. chelonae-abscessus* group. Still, even this methodology cannot differentiate between *M. abscessus, M. bolletii* and *M. massiliense*.[20] There are other databases such as the Ez Taxon identification service (EzTaxon-e) and the basic local alignment search tool (BLAST), but they have no quality control standards for the submission of reference sequences.[35,36]

Identification using other housekeeping gene sequences

The sequence of the 16S rRNA gene (first one-third) cannot identify or differentiate some mycobacterium strains, but the entire gene is relatively large, and large amounts of DNA template are required to obtain the entire sequence. A more sensitive method for the targeting of multiple housekeeping genes

Table 4. Primers used for NTM and *M. ulcerans* detection and identification

Primer	Sequence	Target and/or purpose (amplified fragment size)	Reference
8F16S 1047R16S 830F16S 1542R16S	5′-AGAGTTTGATCCTGGCTCAG-3′ (positions 8 to 27)[a] 5′-TGCACACAGGCCACAAGGGA-3′ (positions 1047 to 1028)[a] 5′-GTGTGGGTTTCCTTCCTTGG-3′ (positions 830 to 849)[a] 5′-AAGGAGGTGATCCAGCCGCA-3′ (positions 1542 to 1523)[a]	Mycobacterial 16S rRNA gene, PCR (1500 bp), sequencing	24
TB11 TB12	5′-ACCAACGATGGTGTGTCCAT-3′ 5′-CTTGTCGAACCGCATACCCT-3′	Mycobacterial *hsp65 gene*, PCR (441 bp), sequencing	25
MabrpoF MabrpoR	5′-GAGGGTCAGACCACGATGAC-3′ (positions 2112–2131)[b] 5′-AGCCGATCAGACCGATGTT-3′ (positions 2559–2541)[b]	Mycobacterial *rpoB gene*, PCR (449 bp), sequencing	20
MF MR	5′-CGACCACTTCGGCAACCG-3′ 5′-TCGATCGGGCACATCCGG-3′	Mycobacterial *rpoB gene*, PCR (341 bp), sequencing	26
ITSF ITSR	5′-TTGTACACACCGCCCGTC-3′ 5′-TCTCGATGCCAAGGCATCCACC-3′	Mycobacterial 16S-23S ITS region, PCR (340 bp), sequencing	27
PU4F PU7Rbio	5′-GCGCAGATCAACTTCGCGGT-3′ 5′-GCCCGATTGGTGCTCGGTCA-3′	*M. ulcerans* IS*2404*, PCR (154 bp)	28

[a]Nucleotide positions were assigned using the coli *E. coli* 16S rRNA gene sequence as a reference.[b]Primer design and nucleotide positions were based on the *M. tuberculosis rpoB* gene sequence (Genbank accession no. L27989). ITS, internal transcribed spacer; PCR, polymerase chain reaction.

Table 5. 16S rRNA gene sequences differentiating *Mycobacterium ulcerans* and related species[19]

Organism	Origin	492[a]	1247	1288	1449–1451
M. ulcerans subsp. *shinshuense* ATCC 33728	Japan	GGGGA	GTGCA	AAGGC	ACCC—TTTG
M. ulcerans subsp. *shinshuense* LRC 0501	Japan	GGGGA	GTGCA	AAGGC	ACCC—TTTG
M. ulcerans ITM 98–912	China	GGGGA	GTGCA	AAGGC	ACCC—TTTG
M. ulcerans Agy99	Ghana	GGAGA	GTGCA	AACGC	ACCCTTTTTTG
M. ulcerans ATCC 19423^T	Australia	GGAGA	GTGCA	AACGC	ACCC—TTTG
M. ulcerans 1615	Malaysia	GGAGA	GTGCA	AACGC	ACCC—TTTG
M. ulcerans 5143	Mexico	GGAGA	GTGCA	AAAGC	ACCC—TTTG
M. marinum ATCC 927^T	USA	GGAGA	GTACA	AAAGC	ACCC—TTTG

[a]Nucleotide position(s) were based on *Escherichia coli* 16S rRNA gene sequence.
Underline indicated differieng residue(s).

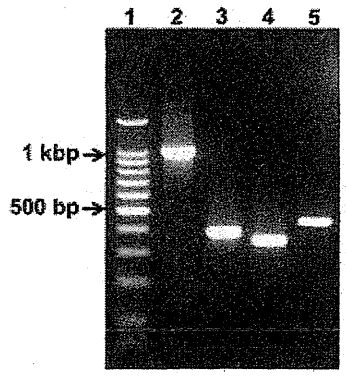

Figure 6. Gel electrophoresis of polymerase chain reaction products from skin biopsy specimens using a 2% agarose gel. Lane 1, 100-bp ladder; lane 2, 16S rRNA gene (8F16S-1047R16S); lane 3, internal transcribed spacer region; lane 4, *rpoB* gene (MF-MR); lane 5, *hsp65* gene.

for PCR and sequence analysis was required.[37] In addition to the 16S rRNA gene, we analyzed the DNA sequences of heat shock protein 65 (*hsp65*), *rpoB* and the 16S–23S intergenic spacer region (ITS region). Table 4 shows the sets of primers applicable to most strains of mycobacterium. Figure 6 shows the result of gel electrophoresis analysis after PCR using template DNA extracted from regions of affected skin and primers for the 16S rRNA gene (8F16S-1047R16S), the ITS region, *rpoB* (MF-MR) and *hsp65*. This figure shows amplified single bands; however, extra bands or inadequate amplification are sometimes apparent. The *rpoB* gene is the most polymorphic of the regions examined and is, therefore, very useful for identification, but the acquisition of PCR products is relatively difficult and the preparation of two different primer sets (MabrpoF-MabrpoR and MF-MR) is required to achieve the desired results. RIDOM database analysis using sequences of the ITS region and the 16S rRNA gene will find strains with higher levels of homology. In contrast, a BLAST search of *rpoB*

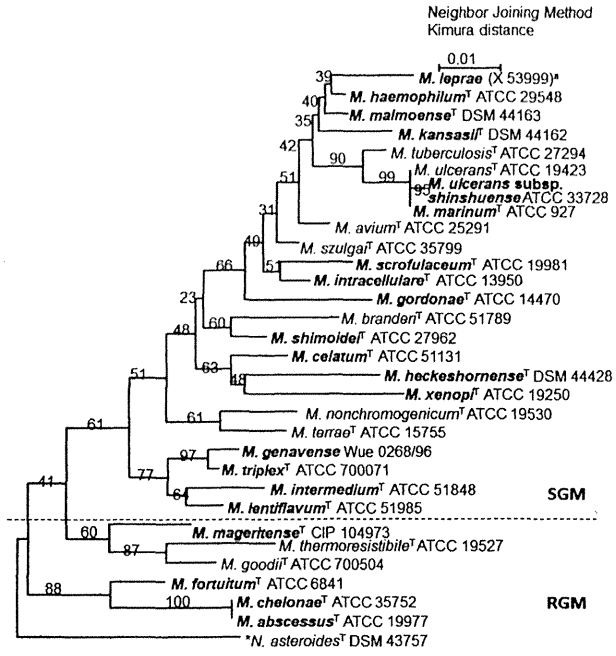

Figure 7. Phylogenetic trees of common pathogenic mycobacteria. A bold letter indicates the species which have been identified in our institute.

and *hsp65* gene would be needed for further consideration. Because quality control is not used in BLAST, care should be taken when it is used as a comparison tool. After the analysis of four different gene sequences, the most homologous bacteria can be chosen as phylogenetic mycobacteria. Sometimes, there is no match to the four different genes, which might be indicative of a novel species.[38] It is recommended that samples be sent to a specialized institution for accurate identification of rare strains.

Phylogenetic trees analysis

Approximately 30 species of mycobacteria have been reported as human pathogens in Japan, and it is assumed that these species cause disease throughout Asia as well. Figure 7 shows a phylogenetic tree of these 30 pathogens based on 16S rRNA sequence data. *M. leprae* is closely related to *Mycobacterium haemophilum*, while *M. ulcerans* subsp. *shinshuense* is a close relative of *M. ulcerans*, *M. marinum* and even *M. tuberculosis*, which are all only distantly related to the RGM species.

Drug susceptibility test

Antibiotic susceptibility profiles are key considerations in the choice of treatment options for mycobacterial infections. Cultured bacteria from cutaneous wounds can be used in susceptibility testing in order to choose antibiotics. The test is performed according to the microdilution method approved by the Clinical Laboratory and Standards Institute (CLSI).[39] In general, microdilution is an easy and reliable technique for this purpose. The approved method was revised recently to state that cation-adjusted Müller–Hinton broth (CAMHB) should be used as culture media for the assay. In particular, CAMHB without OADC supplementation should be used to determine the concentration of drugs against RGM isolates. Mutations in certain genes have been associated with antibiotic resistance (Table 6). Genotypic analysis of these genes can be performed,

Table 6. Drug resistance-related mutations in *Mycbacterium tuberculosis* and other mycobacteria

Drug	Related gene	Gene product
Rifampicin (RFP)	*rpoB*	DNA-dependent RNA polymerase β subunit[40]
Isoniazid (INH)	*katG*	Catalase-peroxidase[41]
	inhA	NADH-dependent enoylacyl carrier protein reductase[42]
	ahpC	Alkyl hydroxyperoxidase[43]
Ethambutol (EB)	*embB*, *embA*, *embC*	Arabinosyl transferase[44]
Pyrazinamide (PZA)	*pncA*	Pyrazinamidase/ nicotinamidase[45]
Streptomycin (SM)	*rpsL*	Ribosomal protein S12[46]
	*r*RNA	16S rRNA[47]
Kanamaycin (KM)	*r*RNA	16S rRNA[48]
Diaminodiphenyl sulfone (DDS, dapsone)	*folP*	Dihydropteroate synthase[49]
Fluoroquinolones	*gyrA*, *gyrB*	DNA gyrase A subunit, B subunit[50]
Clarithromycin (CAM)	*r*RNA	23S rRNA[51]

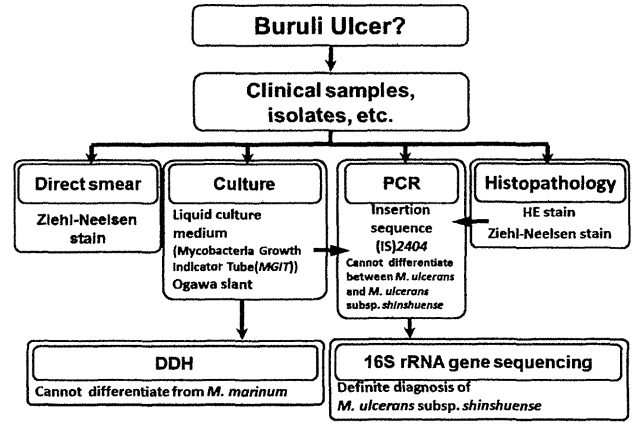

Figure 8. Flow chart for the differential identification of Buruli ulcer. DDA, DNA–DNA hybridization; HE, hematoxylin–eosin; PCR, polymerase chain reaction.

but the process could prove to be very labor intensive in a clinical setting.

CASE STUDY: IDENTIFICATION OF A CUTANEOUS NTM INFECTION

Diagnosis of BU[52–54]

A PCR assay targeting IS*2404* is frequently used to diagnose BU[28] The PCR-amplified sequences of the IS*2404* target are less than 200 bp (Table 4). At present, IS*2404* has been found only in two strains of human pathogenic mycobacteria: *M. ulcerans* and *M. ulcerans* subsp. *shinshuense*. Moreover, it is present at more than 200 copies/genome, so the sensitivity is extremely high and it is suitable for screening and differential identification.[55,56] It is noteworthy that some groups of mycobacterium derived from fish and amphibians also carry IS*2404*,[57–60] therefore, caution must be exercised during environmental studies. Figure 8 shows the flow chart for the diagnosis of BU. It is principally the same as that found in the World Health Organization manual for the diagnosis of *M. ulcerans* disease.[61]

Practical PCR assay using paraffin specimens

DNA should be fragmented when dealing with formalin-fixed paraffin-embedded clinical samples. The amplification of long DNA regions by PCR is often difficult, but assays targeting shorter regions of less than 200 bp are more feasible. The caveat is that detection sensitivity is very low with formalin-fixed paraffin-embedded samples; however, the transport and storage of specimens are relatively easy. In practice, the quality and integrity of DNA from these specimens should be confirmed. Amplification of the β-globin region of human genomic DNA should be used as a control. In Figure 5 (to the left of the marker), lanes 1 and 2 show positive signals for the human β-globin gene, demonstrating that the quality of DNA from the formalin-fixed paraffin-embedded specimens was sufficient for amplification. To the right of the marker lane are amplicons of IS*2404*. Lanes 1 and 2 show a 154-bp band, the right size of the IS*2404* target in *M. ulcerans* and *M. ulcerans* subsp. *shinshuense*. No signal was observed in the negative control (NC) lane, while 154-bp and 205-bp bands appeared in the positive control (PC) lane.

CONCLUSION

At present, 156 species and 13 subspecies of mycobacteria have been registered.[62] New mycobacterial species are being reported because liquid medium is broadly used as the isolation medium, and the ease of isolation from broth culture has increased significantly. Moreover, the progression of genotypic analysis has contributed to this increased rate of discovery. The increase in the number of NTM patients has highlighted the importance of rapid diagnosis of mycobacterial agents.

An elementary, but important, precautionary statement is that specimens should be collected before starting antibiotic treatment. For cases in which the mycobacterium species are rare or are difficult to diagnose, further analysis may be required by a specialized institution.

ACKNOWLEDGMENTS

This work was supported in part by a Grant-in-Aid for Research on Emerging and Re-emerging Infectious Diseases from the Ministry of Health, Labor and Welfare of Japan to Y. H., M. M. and N. I.; a Grant-in-Aid for Scientific Research (C) from the Ministry of Education, Culture, Sports, Science and Technology of Japan for Y. H.; and a Grant-in-Aid for Scientific Research (C) from the Japan Society for the Promotion of Science to K. N.

REFERENCES

1 Liao CH, Lai CC, Ding LW *et al.* Skin and soft tissue infection caused by non-tuberculous mycobacteria. *Int J Tuberc Lung Dis* 2007; **11**: 96–102.
2 Piersimoni C, Scarparo C. Extra pulmonary infections associated with nontuberculous mycobacteria in immunocompetent persons. *Emerg Infect Dis* 2009; **15**: 1351–1358.
3 Lee WJ, Kang SM, Sung H *et al.* Non-tuberculous mycobacterial infections of the skin: a retrospective study of 29 cases. *J Dermatol* 2010; **37**: 965–972.
4 Abbas O, Marrouch N, Kattar MM *et al.* Cutaneous non-tuberculous mycobacterial infections: a clinical and histopathological study of 17 cases from Lebanon. *J Euro Acad Dermatol Venereol* 2011; **25**: 33–42.
5 Chen HY, Chen CY, Huang CT *et al.* Skin and soft-tissue infection caused by non-tuberculous mycobacteria in Taiwan, 1997–2008. *Epidemiol Infect* 2011; **139**: 121–129.
6 Rallis E, Koumantaki-Mathioudaki E. Treatment of *Mycobacterium marinum* cutaneous infections. *Expert Opin Pharmacother* 2007; **8**: 2965–2978.
7 Cheung JP, Fung B, Wong SS, Ip WY. Review article: *Mycobacterium marinum* infection of the hand and wrist. *J Orthopaedic Surg* 2010; **18**: 98–103.
8 Uslan DZ, Kowalski TJ, Wengenack NL, Virk A, Wilson JW. Skin and soft tissue infections due to rapidly growing mycobacteria: comparison of clinical features, treatment, and susceptibility. *Arch Dermatol* 2006; **142**: 1287–1292.
9 Nakanaga K, Hoshino Y, Yotsu RR, Makino M, Ishii N. Nineteen cases of Buruli ulcer diagnosed in Japan from 1980 to 2010. *J Clin Microbiol* 2011; **49**: 3829–3836.
10 Cardoso AM, Sousa EM, Viana-Niero C *et al.* Emergence of nosocomial *Mycobacterium massiliense* infection in Goia's, Brazil. *Microbes Infect* 2008; **10**: 1552–1557.
11 Alinovi A, Vecchini F, Bassissi P. Sporothricoid mycobacterial infection, a case report. *Acta Derm Venereol (Stockh)*, 1993; **73**: 146–147.
12 Kullavanijaya P, Sirimachan S, Bhuddhavudhikrai P. *Mycobacterium marinum* cutaneous infections acquired from occupations and hobbies. *Int J Dermatol*, 1993; **32**: 504–507.
13 Griffith DE, Aksamit T, Brown-Elliott BA *et al.* An official ATS/IDSA statement: diagnosis, treatment, and prevention of nontuberculous mycobacterial diseases. *Am J Respir Crit Care Med* 2007; **175**: 367–416.
14 Della-Latta P, Weitzman I. Mycobacteriology. In: Isenberg HD, ed. *Essential Procedures for Clinical Microbiology*, 1st edn. Washington, DC: ASM Press, 1998; 169–203.
15 Badak FZ, Kiska DL, Setterquist S, Hartley C, O'Connell MA, Hopfer RL. Comparison of mycobacteria growth indicator tube with BACTEC 460 for detection and recovery of mycobacteria from clinical specimens. *J Clin Microbiol* 1996; **34**: 2236–2239.
16 Díaz-Infantes MS, Ruiz-Serrano MJ, Martínez-Sánchez L, Ortega A, Bouza E. Evaluation of the MB/BacT mycobacterium detection system for susceptibility testing of *Mycobacterium tuberculosis*. *J Clin Microbiol* 2000; **38**: 1988–1989.
17 Cohn ML, Waggoner RF, McClatchy JK. The 7H11 medium for the cultivation of mycobacteria. *Am Rev Respir Dis* 1968; **98**: 295–296.

18 Kusunoki S, Ezaki T, Tamesada M *et al.* Application of colorimetric microdilution plate hybridization for rapid genetic identification of 22 mycobacterium species. *J Clin Microbiol* 1991; **29**: 1596–1603.

19 Nakanaga K, Ishii N, Suzuki K *et al.* "*Mycobacterium ulcerans* subsp. *shinshuense*" isolated from a skin ulcer lesion: identification based on 16S rRNA gene sequencing. *J Clin Microbiol* 2007; **45**: 3840–3843.

20 Nakanaga K, Hoshino Y, Era Y *et al.* Multiple cases of cutaneous *Mycobacterium massiliense* infection in a "Hot Spa" in Japan. *J Clin Microbiol* 2011; **49**: 613–617.

21 Chedore P, Jamieson FB. Routine use of the Gen-Probe MTD2 amplification test for detection of *Mycobacterium tuberculosis* in clinical specimens in a large public health mycobacteriology laboratory. *Diagn Microbiol Infect Dis* 1999; **35**: 185–191.

22 Longo MC, Berninger MS, Hartley JL. Use of uracil DNA glycosylase to control carry-over contamination in polymerase chain reactions. *Gene* 1990; **93**: 125–128.

23 Ichimura S, Nagano M, Ito N *et al.* Evaluation of the invader assay with the BACTEC MGIT 960 system for prompt isolation and identification of mycobacterial species from clinical specimens. *J Clin Microbiol* 2007; **45**: 3316–3322.

24 Springer B, Wu WK, Bodmer T *et al.* Isolation and characterization of a unique group of slowly growing mycobacteria: description of *Mycobacterium lentiflavum* sp. nov. *J Clin Microbiol* 1996; **34**: 1100–1107.

25 Telenti A, Marchesi F, Balz M, Bally F, Böttger EC, Bodmer T. Rapid identification of mycobacteria to the species level by polymerase chain reaction and restriction enzyme analysis. *J Clin Microbiol* 1993; **31**: 175–178.

26 Kim BJ, Lee SH, Lyu MA *et al.* Identification of mycobacterial species by comparative sequence analysis of the RNA polymerase gene (*rpoB*). *J Clin Microbiol* 1999; **37**: 1714–1720.

27 Roth A, Fischer M, Hamid ME, Michalke S, Ludwig W, Mauch H. Differentiation of phylogenetically related slowly growing mycobacteria based on 16S-23S rRNA gene internal transcribed spacer sequences. *J Clin Microbiol* 1998; **36**: 139–147.

28 Phillips R, Horsfield C, Kuijper S *et al.* Sensitivity of PCR targeting the IS*2404* insertion sequence of *Mycobacterium ulcerans* in an assay using punch biopsy specimens for diagnosis of Buruli ulcer. *J Clin Microbiol* 2005; **43**: 3650–3656.

29 Turenne CY, Tschetter L, Wolfe J, Kabani A. Necessity of quality-controlled 16S rRNA gene sequence databases: identifying nontuberculous mycobacterium species. *J Clin Microbiol* 2001; **39**: 3637–3648.

30 RIDOM (http://www.ridom-rdna.de/). last accessed 19 October, 2012

31 Harmsen D, Rothgänger J, Frosch M, Albert J. RIDOM: Ribosomal differentiation of medical microorganisms database. *Nucleic Acids Res* 2002; **30**: 416–417.

32 Hall L, Doerr KA, Wohlfiel SL, Roberts GD. Evaluation of the MicroSeq system for identification of mycobacteria by 16S ribosomal DNA sequencing and its integration into a routine clinical mycobacteriology laboratory. *J Clin Microbiol* 2003; **41**: 1447–1453.

33 Kirschner P, Springer B, Vogel U *et al.* Genotypic identification of mycobacteria by nucleic acid sequence determination: report of a 2 year experience in a clinical laboratory. *J Clin Microbiol* 1993; **31**: 2882–2889.

34 Portaels F, Fonteyene PA, de Beenhouwer H *et al.* Variability in 3' end of 16S rRNA sequence of *Mycobacterium ulcerans* is related to geographic origin of isolates. *J Clin Microbiol* 1996; **34**: 962–965.

35 Chun J, Lee JH, Jung Y *et al.* EzTaxon: a web-based tool for the identification of prokaryotes based on 16S ribosomal RNA gene sequences. *Int J Syst Evol Microbiol* 2007; **57**: 2259–2261.

36 Altschul SF, Madden TL, Schaffer AA *et al.* Gapped BLAST and PSI-BLAST: a new generation of protein database search programs. *Nucleic Acids Res* 1997; **25**: 3389–3402.

37 Devulder G, Montclos MP, Flandrois JP. A multigene approach to phylogenetic analysis using the genus mycobacterium as a model. *Int J Syst Evol Microbiol* 2005; **55**: 293–302.

38 Nakanaga K, Hoshino Y, Wakabayashi M *et al. Mycobacterium shigaense* sp. nov., a novel slowly growing scotochromogenic mycobacterium that produced nodules in an erythroderma patient with severe cellular immunodeficiency and a history of Hodgkin's disease. *J Dermatol* 2012; **39**: 389–396.

39 Woods GL, Brown-Elliot BA, Conville PS *et al. Susceptibility Testing of Mycobacteria, Nocardia and other Aerobic Actinomycetes; Approved standard* 2nd edn. The clinical and laboratory standards institute (CLSI), Wayne, PA ; Document No.M24-A2, 2011.

40 Telenti A, Imboden P, Marchesi F *et al.* Detection of rifampicin-resistance mutations in *Mycobacterium tuberculosis*. *Lancet* 1993; **341**: 647–650.

41 Zhang Y, Heym B, Allen B, Young D, Cole S. The catalase-peroxidase gene and isoniazid resistance of *Mycobacterium tuberculosis*. *Nature* 1992; **358**: 591–593.

42 Banerjee A, Dubnau E, Quemard A *et al. inhA*, a gene encoding a target for isoniazid and ethionamide in *Mycobacterium tuberculosis*. *Science* 1994; **263**: 227–230.

43 Wilson TM, Collins DM. *ahpC*, a gene involved in isoniazid resistance of the *Mycobacterium tuberculosis* complex. *Mol Microbiol* 1996; **19**: 1025–1034.

44 Belanger AE, Besra GS, Ford ME *et al.* The *embAB* genes of *Mycobacterium avium* encode an arabinosyl transferase involved in cell wall arabinan biosynthesis that is the target for the antimycobacterial drug ethambutol. *Proc Natl Acad Sci USA* 1996; **93**: 11919–11924.

45 Scorpio A, Zhang Y. Mutations in *pncA*, a gene encoding pyrazinamidase/nicotinamidase, cause resistance to the antituberculous drug pyrazinamide in tubercle bacillus. *Nat Med* 1996; **2**: 662–667.

46 Nair J, Rouse DA, Bai GH, Morris SL. The *rpsL* gene and streptomycin resistance in single and multiple drug-resistant strains of *Mycobacterium tuberculosis*. *Mol Microbiol* 1993; **10**: 521–527.

47 Honoré N, Marchal G, Cole ST. Novel mutation in 16S rRNA associated with streptomycin dependence in *Mycobacterium tuberculosis*. *Antimicrob Agents Chemother* 1995; **39**: 769–770.

48 Heym B, Honoré N, Truffot-Pernot C *et al.* Implications of multidrug resistance for the future of short-course chemotherapy of tuberculosis: a molecular study. *Lancet* 1994; **344**: 293–298.

49 Williams DL, Spring L, Harris E, Roche P, Gillis TP. Dihydropteroate synthase of *Mycobacterium leprae* and dapsone resistance. *Antimicrob Agents Chemother* 2000; **44**: 1530–1537. Erratum in: *Antimicrob Agents Chemother* 2001; **45**: 647.

50 Takiff HE, Salazar L, Guerrero C *et al.* Cloning and nucleotide sequence of *Mycobacterium tuberculosis gyrA* and *gyrB* genes and detection of quinolone resistance mutations. *Antimicrob Agents Chemother* 1994; **38**: 773–780.

51 Wallace RJ Jr, Meier A, Brown BA *et al.* Genetic basis for clarithromycin resistance among isolates of *Mycobacterium chelonae* and *Mycobacterium abscessus*. *Antimicrob Agents Chemother* 1996; **40**: 1676–1681.

52 Portaels F, Silva MT, Meyers WM. Buruli ulcer. *Clin Dermatol* 2009; **27**: 291–305.

53 Walsh DS, Portaels F, Meyers WM. Buruli ulcer: advances in understanding *Mycobacteriumulcerans* infection. *Dermatol Clin* 2011; **29**: 1–8.

54 Yotsu RR, Nakanaga K, Hoshino Y, Suzuki K, Ishii N. Buruli ulcer and current situation in Japan: a new emerging cutaneous mycobacterium infection. *J Dermatol* 2012; **39**: 587–593.

55 Stinear T, Ross BC, Davies JK *et al.* Identification and characterization of IS*2404* and IS*2606*: two distinct repeated sequences for detection of *Mycobacterium ulcerans* by PCR. *J Clin Microbiol* 1999; **37**: 1018–1023.

56 Stinear T, Davies JK, Jenkin GA *et al.* A simple PCR method for rapid genotype analysis of *Mycobacterium ulcerans*. *J Clin Microbiol* 2000; **38**: 1482–1487.

57 Stragier P, Hermans K, Stinear T, Portaels F. First report of a mycolactone-producing mycobacterium infection in agriculture in Belgium. *FEMS Microbiol Lett* 2008; **286**: 93–95.

58 Mve-Obiang A, Lee RE, Umstot E *et al.* A newly discovered mycobacterial pathogen isolated from laboratory colonies of *xenopus* species with lethal infections produces a novel form of mycolactone, the *Mycobacterium ulcerans* macrolide toxin. *Infect Immun* 2005; **73**: 3307–3312.
59 Rhodes M, Kator H, McNabb A *et al. Mycobacterium pseudoshottsii* sp. nov., a slowly growing chromogenic species isolated from Chesapeake Bay striped bass (*Morone saxatilis*). *Int J Syst Evol Microbiol* 2005; **55**: 1139–1147.
60 Ranger BS, Mahrous EA, Mosi L *et al.* Globally distributed mycobacterial fish pathogens produce a novel plasmid-encoded toxic macrolide, mycolactone F. *Infect Immun* 2006; **74**: 6037.
61 World Health Organization. Buruli ulcer: diagnosis of *Mycobacterium ulcerans* disease: a manual for health care providers. In: Portaels F, Johnson P, Meyers WM, published in Apr. 2001. (http://whqlibdoc.who.int/hq/2001/WHO_CDS_CPE_GBUI_2001.4.pdf).
62 List of Prokaryotic names with Standing in Nomenclature (http://www.bacterio.cict.fr/, last accessed 19 October 2012).

RESEARCH ARTICLE

Clofazimine Modulates the Expression of Lipid Metabolism Proteins in *Mycobacterium leprae*-Infected Macrophages

Yang Degang[1,2], Takeshi Akama[1], Takeshi Hara[1], Kazunari Tanigawa[1], Yuko Ishido[1], Masaichi Gidoh[1], Masahiko Makino[1], Norihisa Ishii[1], Koichi Suzuki[1*]

1 Leprosy Research Center, National Institute of Infectious Diseases, Higashimurayama, Tokyo, Japan, **2** Department of Leprosy and Infectious Diseases, Shanghai Skin Disease Hospital, Shanghai, China

Abstract

Mycobacterium leprae (M. leprae) lives and replicates within macrophages in a foamy, lipid-laden phagosome. The lipids provide essential nutrition for the mycobacteria, and *M. leprae* infection modulates expression of important host proteins related to lipid metabolism. Thus, *M. leprae* infection increases the expression of adipophilin/adipose differentiation-related protein (ADRP) and decreases hormone-sensitive lipase (HSL), facilitating the accumulation and maintenance of lipid-rich environments suitable for the intracellular survival of *M. leprae*. HSL levels are not detectable in skin smear specimens taken from leprosy patients, but re-appear shortly after multidrug therapy (MDT). This study examined the effect of MDT components on host lipid metabolism *in vitro*, and the outcome of rifampicin, dapsone and clofazimine treatment on ADRP and HSL expression in THP-1 cells. Clofazimine attenuated the mRNA and protein levels of ADRP in *M. leprae*-infected cells, while those of HSL were increased. Rifampicin and dapsone did not show any significant effects on ADRP and HSL expression levels. A transient increase of interferon (IFN)-β and IFN-γ mRNA was also observed in cells infected with *M. leprae* and treated with clofazimine. Lipid droplets accumulated by *M. leprae*-infection were significantly decreased 48 h after clofazimine treatment. Such effects were not evident in cells without *M. leprae* infection. In clinical samples, ADRP expression was decreased and HSL expression was increased after treatment. These results suggest that clofazimine modulates lipid metabolism in *M. leprae*-infected macrophages by modulating the expression of ADRP and HSL. It also induces IFN production in *M. leprae*-infected cells. The resultant decrease in lipid accumulation, increase in lipolysis, and activation of innate immunity may be some of the key actions of clofazimine.

Author Summary

Leprosy, caused by *Mycobacterium leprae (M. leprae)*, is an ancient infectious disease that remains the leading infectious cause of disability. After infection, *M. leprae* lives inside host macrophages that contain a large amount of lipids, which is thought to be an essential microenvironment for *M. leprae* to survive in host cells. *M. leprae* infection increases lipid accumulation in macrophages and decreases the metabolic breakdown of lipids (catabolism). In addition, the treatment of leprosy with multidrug therapy (MDT) reverses the effect of infection

on the modulation of lipid metabolism. We therefore aimed to use cultured human macrophage cells to determine which of the three MDT drugs (clofazimine, dapsone, or rifampicin) is responsible for this effect. We found that only clofazimine affects lipid accumulation and catabolism in *M. leprae*-infected cells *in vitro*. The amounts of lipids accumulated in the cells decreased when clofazimine was added to the cell culture medium. Clofazimine also activated immune responses in *M. leprae*-infected cells. These results suggest that the effectiveness of clofazimine against leprosy is due to the modulation of lipid metabolism and activation of immune reactions in *M. leprae*-infected host cells.

Citation: Degang Y, Akama T, Hara T, Tanigawa K, Ishido Y, et al. (2012) Clofazimine Modulates the Expression of Lipid Metabolism Proteins in *Mycobacterium leprae*-Infected Macrophages. PLoS Negl Trop Dis 6(12): e1936. doi:10.1371/journal.pntd.0001936

Editor: Joseph M. Vinetz, University of California San Diego School of Medicine, United States of America

Received: August 1, 2012; **Accepted:** October 20, 2012; **Published:** December 6, 2012

Funding: This work was supported by a Grant-in-Aid for Scientific Research (C) from the Japan Society for the Research Promotion of Science (#23803000; http://www.jsps.go.jp/j-grantsinaid/index.html). The funder had no role in study design, data collection and analysis, decision to publish, or preparation of the manuscript.

Competing interests: The authors have declared that no competing interests exist.

* E-mail: koichis@nih.go.jp

INTRODUCTION

Leprosy is a chronic infectious disease caused by *Mycobacterium leprae* (*M. leprae*), which is a typical intracellular pathogen that parasitizes tissue macrophages (histiocytes) and Schwann cells of the peripheral nerves of the dermis. Although its prevalence has declined over the last several decades due to the introduction of multi-drug therapy (MDT) by the World Health Organization (WHO), leprosy remains a major public health problem in many developing countries: In 2010, 228,474 new cases were registered worldwide [1]. Based on their clinical, histological and immunological manifestations, leprosy patients are classified into five groups that comprise one continuous spectrum: Tuberculoid (TT), Borderline Tuberculoid (BT), Borderline (BB), Borderline Lepromatous (BL) and Lepromatous (LL) [2]. LL is characterized by widespread skin lesions containing numerous bacilli that live in the foamy or enlarged lipid-filled phagosome within macrophages. Schwann cells in LL nerves also have the foamy, lipid-laden appearance that favors mycobacterial survival and persistence. In Schwann cells, *M. leprae* infection-induced biogenesis of lipid droplets correlates with increased prostaglandin E2 (PGE2) and interleukin-10 (IL-10) secretion, which is essential for leprosy pathogenesis [3], [4]. Although lipid-laden macrophages

are also observed in other mycobacterial infections, including tuberculosis [5], [6], the amount of lipid and the number of infected macrophages are most prominent in cases of LL [7], [8].

The PAT protein family is named after three of its members: perilipin, adipophilin/adipose differentiation-related protein (ADRP), and tail-interacting protein of 47 kDa (TIP47). PAT family members are responsible for the transportation of lipids and the formation of lipid droplets in a variety of tissues and cultured cell lines, including adipocytes [9]–[12]. ADRP selectively increases the uptake of long chain fatty acids and has an essential role in fatty acid transport [13], [14]. Hormone-sensitive lipase (HSL), as the first enzyme identified in the induction of lipo-catabolic action initiated by hormones, is the predominant lipase effector of catecholamine-stimulated lipolysis in adipocytes [15]. Therefore, ADRP and HSL have opposing functions, i.e., lipid accumulation vs. its degradation. ADRP and HSL also play important roles in lipid accumulation in *M. leprae*-infected macrophages [8], [16]. *M. leprae* infection increased the expression of ADRP mRNA and protein, facilitating the accumulation and maintenance of a lipid-rich environment suitable for intracellular survival [8]. Conversely, HSL expression was suppressed in macrophages infected with *M. leprae* [16]. These results suggest that both ADRP and HSL influence the lipid-rich environment that favors *M. leprae* parasitization and survival in infected host cells. In our previous study, HSL expression was not detectable in slit-skin smear specimens from non-treated LL and BL patients, but it re-appeared shortly after MDT treatment [16]. However, how treatment modulates HSL expression is not clear. In the present study, we determine the effect of MDT components on host lipid metabolism by investigating the influence of rifampicin, dapsone and clofazimine on the expression of ADRP and HSL in THP-1 cells.

MATERIALS AND METHODS

Ethic statement

Human specimens were used according to the guidelines approved by the Ethical Committee of the National Institute of Infectious Diseases (Tokyo, Japan). All samples were anonymized before use.

Drugs

Clofazimine (Sigma-Aldrich Co., St. Louis, MO), rifampicin (Wako Pure Chemical Industries Ltd., Osaka, Japan) and dapsone (Wako Pure Chemical Industries Ltd.) were dissolved in dimethyl sulfoxide (DMSO) and stored at 4°C. The final concentration used in the culture medium was 8.0 μg/ml rifampicin, 5.0 μg/ml dapsone or 2.0 μg/ml clofazimine.

M. leprae isolation and cell culture

Hypertensive nude rats (SHR/NCrj-rnu), infected with the Thai53 strain of *M. leprae* [17], [18] were kindly provided by Dr. Y. Yogi of the Leprosy Research Center, National Institute of Infectious Diseases. Japan. The protocol was approved by the Experimental Animal Committee, of the National Institute of Infectious Diseases, Tokyo, Japan (Permit Number: 206055). Animal studies were carried out in strict accordance with the recommendations from Japan's Animal Protection Law. *M. leprae* was isolated as previously described [19], [20]. The human premonocytic cell line THP-1 was obtained from the American Type Culture Collection (ATCC; Manassas, VA). The cells were cultured in six-well plates in RPMI medium supplemented with 10% charcoal-treated fetal bovine serum (FBS), 2% non-essential amino acids, 100 IU/ml penicillin and 100 μg/ml streptomycin at 37°C in

5% CO_2 [7], [8]. Typically, 3×10^7 bacilli were added to 3×10^6 THP-1 cells (multiplicity of infection: MOI = 10).

RNA preparation and reverse transcription polymerase chain reaction (RT-PCR)

Total RNA from cultured cells was prepared using RNeasy Mini Kits (Qiagen Inc., Valencia, CA) as described previously [7], [8]. Total RNA preparation from slit-skin smear samples was performed as described [8], [16]. Briefly, stainless steel blades (Feather Safety Razor Co., Osaka, Japan) used to obtain slit-skin smear specimens were rinsed in 1 ml of sterile 70% ethanol. The tube was then centrifuged at 20,000×g for 1 min at 4°C. After removing the supernatant, RNA was purified with the same protocol that was used for cultured cells. The RNA was eluted in 20 µl of elution buffer and treated with 0.1 U/µl DNase I (TaKaRa Bio, Kyoto, Japan) at 37°C for 60 min to degrade any contaminating genomic DNA. All RNA samples had an OD260/280 of 1.8–2.0 and an OD260/230 >1.8. RNA sample quality was also confirmed using denaturing agarose gel electrophoresis and the Agilent 2100 Bioanalyzer (Agilent Technologies, Santa Clara, CA) (**Fig. S1**). Total RNA from each sample was reverse-transcribed to cDNA using a High Capacity cDNA Reverse Transcription Kit (Applied Biosystems, Foster City, CA) with random primers [8], [16]. The following primers were used to amplify specific cDNAs: ADRP: 5′-TGTGGAGAAGACCAAGTCTGTG-3′ (forward) and 5′-GCTTCTGAACCAGATCAAATCC-3′ (reverse); HSL: 5′-CTCCTCATGGCTCAACTCCTTCC-3′ (forward) and 5′-AGGGGTTCTTGACTATGGGTG-3′ (reverse); interferon (IFN)-β: 5′-TGCTCTCCTGTTGTGCTTCTCCAC-3′ (forward) and 5′-CAATAGTCTCATTCCAGCCAGTGC-3′ (reverse); IFN-γ: 5′-GCAGAGCCAAATTGTCTCCTTTTAC-3′ (forward) and 5′-ATGCTCTTCGACCTCGAAACAGC-3′ (reverse) and actin: 5′-AGCCATGTACGTAGCCATCC-3′ (forward) and 5′-TGTGGTGGTGAAGCTGTAGC-3′ (reverse). Touchdown PCR was performed using a PCR Thermal Cycler DICE (TaKaRa Bio, Tokyo, Japan) [7], [8]. Briefly, the PCR mixture was first denatured for 5 min at 94°C, followed by 20 cycles of three-temperature PCR consisting of a 30-sec denaturation at 94°C, a 30-sec annealing that started at 65°C and decreased 0.5°C every cycle to 55°C, and a 45-sec extension at 72°C. An additional 10 cycles were performed for ADRP and β-actin, and 14 cycles for HSL with a fixed annealing temperature of 55°C. The products were analyzed by 2% agarose gel electrophoresis.

Protein preparation and Western blot analysis

Cellular protein was extracted and analyzed as previously described [16], [21]. Briefly, cells were lysed in a lysis buffer containing 50 mM HEPES, 150 mM NaCl, 5 mM EDTA, 0.1% NP40, 20% glycerol, and protease inhibitor cocktail (Complete Mini, Roche, Indianapolis, IN) for 1 h. After centrifugation, the supernatant was transferred and 10 µg of protein was used for analysis. Cellular proteins were mixed with 4× LDS sample buffer and 10× reducing agent (Invitrogen, Life Technologies, Carlsbad, CA) and incubated for 10 min at 70°C prior to electrophoresis. Proteins were separated on NuPage 4–12% Bis Tris Gels and transferred using an iBlot Gel Transfer Device (Invitrogen). The membrane was washed with PBST (phosphate buffered saline (PBS) with 0.1% Tween 20), blocked in blocking buffer (PBST containing 5% skim milk) overnight, and then incubated with either rabbit anti-ADRP antibody (Santa Cruz Biotechnology Inc., Santa Cruz, CA; 1:2,000 dilution), rabbit anti-HSL antibody (Cell Signaling Technology, Danvers, MA; 1:1,000 dilution) or goat anti-β-actin antibody (Santa Cruz; dilution 1:2,000). After washing with PBST, the membrane was incubated for 1 h with biotinylated donkey anti-rabbit antibody for ADRP and HSL (GE Healthcare, Fairfield, CT; 1:2,000 dilution) or biotinylated donkey anti-goat antibody for β-actin

(Millipore, Billerica, MA; dilution 1:10,000) followed by streptavidin-HRP (GE Healthcare; 1:10,000 dilution) for 1 h. The signal was developed using ECL Plus Reagent (GE Healthcare).

Lipid staining

THP-1 cells were grown on glass coverslips in 24-well plates for 24 h, before the culture medium was exchanged with RPMI 1640 containing *M. leprae* and clofazimine. Control and drug-treated THP -1 cells were fixed in 10% formalin for 10 min. They were then washed with Dulbecco's PBS (DPBS) and balanced with 60% isopropanol for 1 min before staining with oil-red-O (Muto Pure Chemicals, Tokyo, Japan) for 10 min. The cells were counterstained with hematoxylin for 5 min followed by ethanol dehydration and coverslip sealing.

Immunohistochemistry

Archived formalin-fixed, paraffin-embedded tissue sections were subjected to immunohistochemical staining as described [7]. Briefly, deparaffinized sections were heated in 1 mM NaOH at 120°C for 5 min for antigen retrieval. They were then washed with PBST and blocked in blocking buffer (DAKO, Carpinteria, CA) for 10 min, and then incubated with either anti-ADRP antibody (Santa Cruz Biotechnology Inc.; 1:200 dilution) or anti-HSL antibody (Cell Signaling Technology; 1:100 dilution), for 1 h at room temperature. After washing the slides with PBST, peroxidase-labeled streptavidin-biotin method was employed using the LSAB2 kit (DAKO) and 3,3-diaminobenzidine tetrahydrochloride (DAB) for the staining of ADRP. Tyramide signal amplification (TSA)-HRP method was utilized to amplify HSL staining signals using the TSA Biotin System (PerkinElmer, Inc., Waltham, MA) according to the manufacturer's protocol. Sections were then stained using carbol fuchsin to visualize acid-fast mycobacteria and counterstained with hematoxylin.

Others

All experiments were repeated at least three times. Since the replicates produced essentially the same outcomes, representative results from these independent experiments are shown in the figures.

RESULTS

Clofazimine decreases ADRP and increases HSL mRNA levels in macrophages infected with *M. leprae*

The effect of MDT drugs on lipid metabolism in *M. leprae*-infected macrophages was examined by infecting human premonocytic THP-1 cells with *M. leprae* (MOI = 10) in the presence of 8.0 μg/ml rifampicin, 5.0 μg/ml dapsone or 2.0 μg/ml clofazimine for 24 h. Total RNA was isolated and RT-PCR analysis was performed to evaluate possible changes in ADRP and HSL mRNA levels. In our previous studies, *M. leprae* infection has been shown to increase ADRP and decrease HSL expression, which will in turn increase the lipid accumulation that is thought to contribute to maintaining a phagosome environment which permits *M. leprae* to parasitize tissue macrophages [8], [16]. However, when *M. leprae*-infected THP-1 cells were treated with clofazimine, ADRP expression levels decreased and HSL expression increased (**Fig. 1**). Rifampicin and dapsone did not show significant effects on the mRNA expression of ADRP, while they decreased HSL expression by augmenting the effect of *M. leprae* infection.

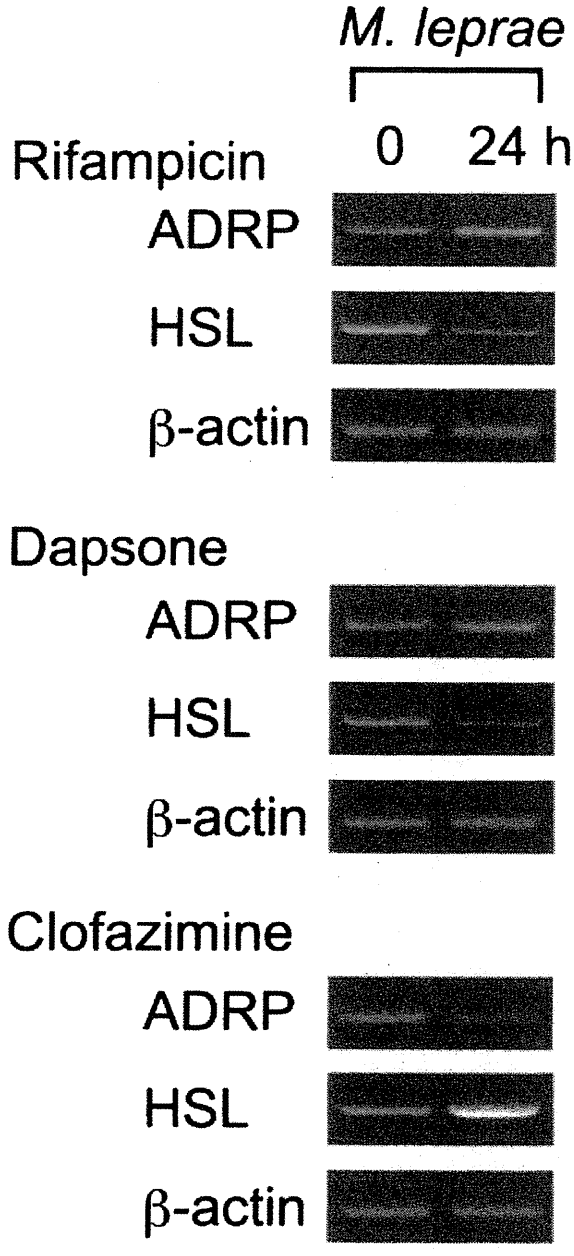

Figure 1. Expression of ADRP and HSL is modulated by clofazimine in THP-1 cells infected with *M. leprae*.

THP-1 cells were cultured in six-well plates with culture medium containing either 8.0 μg/ml rifampicin, 5.0 μg/ml dapsone or 2.0 μg/ml clofazimine with *M. leprae* infection (MOI = 10). After incubating for 24 h, total RNA was purified and RT-PCR analysis of ADRP, HSL and β-actin was performed. Representative results from three independent experiments are shown.

doi:10.1371/journal.pntd.0001936.g001

- **Download:** PowerPoint slide | larger image (114KB PNG) | original image (163KB TIFF)

The effect of clofazimine is specific only for *M. leprae*-infected cells

To further evaluate the effect of clofazimine on ADRP and HSL expression, THP-1 cells were treated with clofazimine in the presence or absence of *M. leprae* infection for 6, 12, 24 and 48 h. Total RNA and cellular protein were extracted and used for RT-PCR analysis and Western blot analysis, respectively. Linearity of the RT-PCR amplifications of ADRP, HSL and β-actin was confirmed by serial dilution of RNA samples and densitometric analysis of the bands (Fig. S2). RT-PCR showed that clofazimine alone had no effect on ADRP and HSL mRNA levels in control THP-1 cells (Fig. 2, left panel). Consistent with previous reports, ADRP mRNA expression was increased and HSL mRNA expression was decreased when THP-1 cells were infected with *M. leprae* (Fig. 2, middle panel) [8],

[16]. However, simultaneous clofazimine treatment and *M. leprae* infection of THP-1 cells led to decreased ADRP and increased HSL mRNA levels (Fig. 2, right panel). The decrease of ADRP and increase of HSL mRNA expression were further confirmed by quantitative real-time PCR (Fig. S3), which also supports the linearity of our RT-PCR data. Thus, it was shown that clofazimine modulated expression of ADRP and HSL only in *M. leprae*-infected cells. Similar results were observed for ADRP and HSL protein expression levels in each experiment.

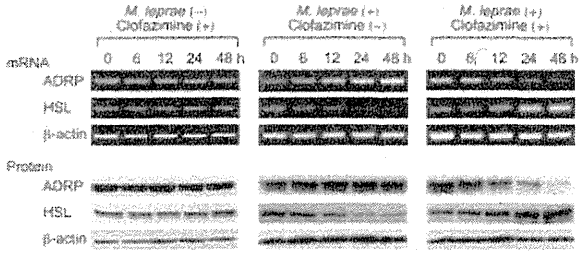

Figure 2. Only *M. leprae*-infected THP-1 cells are susceptible to clofazimine.

THP-1 cells were cultured in six-well plates with or without 2.0 μg/ml clofazimine in the presence or absence of *M. leprae* infection (MOI = 10). After incubating for the indicated period of time, total RNA and total cellular protein were purified and RT-PCR and Western blot analyses of ADRP, HSL and β-actin were performed. Representative results from three independent experiments are shown.

doi:10.1371/journal.pntd.0001936.g002

- **Download:** PowerPoint slide | larger image (465KB PNG) | original image (607KB TIFF)

Clofazimine antagonizes the effects of *M. leprae* to modulate ADRP and HSL expression

In the above studies, THP-1 cells were simultaneously treated with clofazimine and infected with *M. leprae*. Therefore, there was a possibility that clofazimine might have modulated the cellular environments of THP-1 cells before engulfing *M. leprae*. To eliminate this possibility and to imitate clinical situations, THP-1 cells were first infected with *M. leprae* for 24 h, to allow cells to engulf enough bacilli, before they were treated with clofazimine. *M. leprae* infection enhanced ADRP expression and suppressed HSL expression for up to 72 h (Fig. 3, left panel), which is consistent with the results shown in Fig. 2, middle panel. However, adding clofazimine 24 h after *M. leprae* infection produced lower levels of ADRP expression, but increased HSL expression (Fig. 3, right panel). Interestingly, ADRP expression fell even lower than the original level, and HSL rose higher than original levels, following clofazimine treatment. These results suggest that the lipid catabolic activity once suppressed by *M. leprae* infection was reactivated by clofazimine treatment, which in turn would promote lipolysis in infected macrophages and decrease cellular lipids. Also, these results are consistent with clinical situations in which HSL mRNA levels were recovered following successful treatment with MDT in LL and BL patients [16].

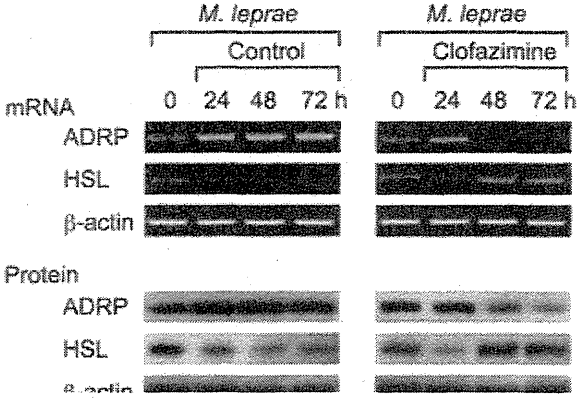

Figure 3. Clofazimine counteracts *M. leprae* to modulate ADRP and HSL expression levels.

THP-1 cells were cultured in six-well plates and infected with *M. leprae* (MOI = 10) for 24 h. Clofazimine (2.0 μg/ml) was added and incubation continued another 24 and 48 h (48 and 72 h from *M. leprae* infection). Total RNA and total cellular protein were purified and RT-